Organometallics 1989, *8*, 893–899

Nucleophilic Properties and Electrochemistry of Five-Coordinate Rhodium(I) σ-Cyanide Complexes. Synthesis and Characterization of Stable Cis Hydride Cyanide Complexes of Rhodium(III)

Claudio Bianchini,*[,†] Franco Laschi,[‡] M. Francesca Ottaviani,[§] Maurizio Peruzzini,[†]
Piero Zanello,[‡] and Fabrizio Zanobini[†]

Istituto per lo Studio della Stereochimica ed Energetica dei Composti di Coordinazione, CNR, Via J. Nardi, 39, 50132 Firenze, Italy, Dipartimento di Chimica, Università di Siena, 53100 Siena, Italy, and Dipartimento di Chimica, Università di Firenze, 50100 Firenze, Italy

Received June 17, 1988

The trigonal-bipyramidal (TBP) σ-cyanide complexes of rhodium(I), [(L)Rh(CN)] [L = $N(CH_2CH_2PPh_2)_3$, 1; $P(CH_2CH_2PPh_2)_3$, 2], have been synthesized and spectroscopically characterized. The redox properties of both compounds have been studied in detail and compared with those of the σ-acetylide congeners [(L)Rh(C≡CR)] (R = Ph, CO_2Et). One-electron oxidation of 1 and 2 yields the stable paramagnetic Rh(II) derivatives $[(L)Rh(CN)]^+$ which exhibit square-pyramidal structures as determined by ESR spectroscopy. One-electron oxidation of the Rh(II) compounds gives unstable Rh(III) species of formula $[(L)Rh(CN)]^{2+}$ which readily decompose to the dicyano complexes $[(L)Rh(CN)_2]^+$. Electrophilic attack by Me^+ on 1 and 2 occurs at the nitrogen atom of the σ-bonded cyanide group to give the TBP methyl isocyanide complexes $[(L)Rh(CNMe)]^+$. In contrast, protonation of 1 and 2 takes place at the metal, and the stable, octahedral cis hydride cyanide complexes $[(L)Rh(H)(CN)]^+$ form.

Introduction

As a part of our studies on electron-rich transition-metal complexes with tripodal polyphosphine ligands, we have recently focused much of our attention on a family of neutral, trigonal-bipyramidal (TBP) Rh(I) derivatives of formula [(L)Rh(σ-R)] [L = NP_3, $N(CH_2CH_2PPh_2)_3$; PP_3, $P(CH_2CH_2PPh_2)_3$; R = halide, hydride, alkyl, aryl, acyl].[1] In all of these compounds, the metal center is highly basic and susceptible to attack by electrophiles such as H^+ or alkyl$^+$, thus forming octahedral (OCT) Rh(III) derivatives in which the hydride (or alkyl) and R coligands are forced by the particular geometry of the tripodal ligand to lie in mutually cis positions. The electrons that populate the frontier σ orbital responsible for the nucleophilic character of the metal in these d^8-L_5M systems[2] can also be removed, totally or partially, by chemical or electrochemical oxidation.[1c] In this way, Rh(II) and Rh(III) derivatives of formulas $[(L)Rh(\sigma\text{-}R)]^+$ and $[(L)Rh(\sigma\text{-}R)]^{2+}$, respectively, have been obtained. When the R ligand contains a nucleophilic center within its structure as in the case of σ-acetylide,[1c] there is competition between the metal and the ligand in undergoing electrophilic attack. As an example, [(NP_3)Rh(C≡CPh)], in which the β-carbon of the acetylide ligand is a nucleophilic site, reacts with H^+ in THF or benzene forming the vinylidene complex $[(NP_3)Rh(C{=}CHPh)]^+$.[1c] On the other hand, when the reaction of the PP_3 analogue [(PP_3)Rh(C≡CPh)] is carried out in benzene, the oxidation of the metal prevails over vinylidene formation and the Rh(II) acetylide $[(PP_3)Rh(C{\equiv}CPh)]^+$ is obtained.[3] It is therefore apparent that a subtle balance of several factors, including redox potentials, solvent, and nature of the electrophilic reagent and of the eventual nucleophilic site on the R coligand decides which of the possible reaction pathways prevails over the others, i.e. electrophilic attack at the metal to form OCT Rh(III) complexes, electrophilic attack at the σ-ligand to give TBP Rh(I) complexes, or metal oxidation to yield Rh(II) and Rh(III) derivatives.

In order to gain further insight into the factors that govern the reactions of multinucleophilic transition-metal complexes with electrophiles, we decided to investigate the chemistry and the electrochemistry of the σ-cyanide complexes [(NP_3)Rh(CN)] (1) and [(PP_3)Rh(CN)] (2). Like their acetylide congeners, 1 and 2 possess two potentially nucleophic sites, namely, the metal and the nitrogen atom of the cyano group.

Results and Discussion

Synthesis and Characterization of 1 and 2. The TBP rhodium hydrides [(NP_3)RhH] (3)[1d] and [(PP_3)RhH] (4)[1d] react in THF at 40 °C with excess ethyl cyanoformate, $NCCO_2Et$, yielding ethyl formate and the yellow cyano complexes 1 and 2, respectively (eq 1). The use of $NCCO_2Et$ as starting material to introduce cyanide ligands into complex frameworks has some precedent.[4] It is generally agreed that the reactions proceed through oxidative cleavage of the C–C bond at the metal to give ethoxycarbonyl cyanide complexes. When hydride ligands are present, the reductive elimination of ethyl formate may follow and cyanide complexes form.[4]

$$[(L)RhH] + NCCO_2Et \rightarrow [(L)Rh(CN)] + HCO_2Et \quad (1)$$

An alternative two-step route by which 1 and 2 can be prepared is the one shown in (eq 2). This involves methylation by $MeOSO_2CF_3$ of 3 and 4 in THF to give, via reductive elimination of methane from unstable cis hydride

---

[†] ISSECC, CNR.
[‡] University of Siena.
[§] University of Firenze.

(1) (a) Bianchini, C.; Meli, A.; Peruzzini, M.; Zanobini, F. *J. Chem. Soc., Chem. Commun.* 1987, 971. (b) Bianchini, C.; Meli, A.; Peruzzini, M.; Vacca, A.; Zanobini, F. *Organometallics* 1987, *6*, 2453. (c) Bianchini, C.; Laschi, F.; Ottaviani, M. F.; Peruzzini, M.; Zanello, P. *Ibid.* 1988, *7*, 1660. (d) Bianchini, C.; Masi, D.; Meli, A.; Peruzzini, M.; Zanobini, F. *J. Am. Chem. Soc.* 1988, *110*, 6411. (e) Bianchini, C.; Mealli, C.; Peruzzini, M.; Zanobini, F. *J. Am. Chem. Soc.* 1987, *109*, 5548. (f) Bianchini, C.; Mealli, C.; Meli, A.; Peruzzini, M.; Vizza, F.; Zanobini, F. *J. Organomet. Chem.* 1988, *346*, C53. (g) Bianchini, C.; Peruzzini, M.; Vizza, F.; Zanobini, F. *J. Organomet. Chem.* 1988, *348*, C9.

(2) Bianchini, C.; Meli, A.; Dapporto, P.; Tofanari, A.; Zanello, P. *Inorg. Chem.* 1987, *26*, 3677.

(3) Bianchini, C.; Peruzzini, M., unpublished results.

(4) Bianchini, C.; Masi, D.; Meli, A.; Sabat, M. *Organometallics* 1986, *5*, 1670.

0276-7333/89/2308-0893$01.50/0

Table I. NMR Spectral Characterization for the Complexes[a]

complex	NMR	chem shifts, ppm		coupling constants, Hz	
1	$^{31}P\{^1H\}^b$	$\delta(P)$	28.36 (d)	$J(PRh)$	155.4
2	$^{31}P\{^1H\}$	$\delta(P_A)$	152.07 (dq)	$J(P_AP_M)$	23.1
				$J(P_ARh)$	93.0
		$\delta(P_M)$	50.38 (dd)	$J(P_MRh)$	145.4
8	$^{31}P\{^1H\}$	$\delta(P)$	35.11 (d)	$J(PRh)$	141.4
	$^1H^C$	δ(CNMe)	3.36 (dq)	$^5J(HP)$	3.0
				$^4J(HRh)$	0.8
9	$^{31}P\{^1H\}$	$\delta(P_A)$	149.80 (dq)	$J(P_AP_M)$	23.7
				$J(P_ARh)$	90.2
		$\delta(P_M)$	56.35 (dd)	$J(P_MRh)$	138.1
	^1H	δ(CNMe)	3.30 (dq)	$^5J(HP)$	2.7
				$^4J(HRh)$	0.7
10[d]	$^{31}P\{^1H\}$	$\delta(P)$	25.82 (d)	$J(PRh)$	147.2
	^1H	δ(NCMe)	2.44 (q)	$^5J(HP)$	2.6
11[d]	$^{31}P\{^1H\}$	$\delta(P_A)$	142.83 (dq)	$J(P_AP_M)$	17.9
				$J(P_ARh)$	116.9
		$\delta(P_M)$	47.75 (dd)	$J(P_MRh)$	143.6
	^1H	δ(NCMe)	2.04 (q)	$^5J(HP)$	2.4
12	$^{31}P\{^1H\}$	$\delta(P_A)$	24.84 (dt)	$J(P_AP_M)$	18.1
				$J(P_ARh)$	81.8
		$\delta(P_M)$	42.40 (dd)	$J(P_MRh)$	95.3
	^1H	δ(RhH)	−7.22 (ddt)	$J(HP_{trans})$	166.9
				$J(HP_{cis})$	6.9
				$J(HRh)$	13.7
13	$^{31}P\{^1H\}$	$\delta(P_A)$	137.36 (dpq)	$J(P_AP_M)$	8.7
				$J(P_AP_Q)$	8.7
				$J(P_ARh)$	78.8
		$\delta(P_M)$	47.90 (ddd)	$J(P_MP_Q)$	16.7
				$J(P_MRh)$	94.2
		$\delta(P_Q)$	41.60 (dtd)	$J(P_QRh)$	75.3
	^1H	δ(RhH)	−9.15 (ddpq)	$J(HP_{trans})$	152.2
				$J(HP_{cis})$	10.9
				$J(HRh)$	15.1

[a] 298 K, CD_2Cl_2 solutions, unless otherwise stated. [b] The chemical shifts are relative to H_3PO_4 (85%), with positive values being downfield from the standard. Key: d, doublet; t, triplet, q, quartet; pq, pseudoquartet. [c] The chemical shifts are relative to TMS. The resonance due to the hydrogen atoms belonging to the tripodal ligands are not reported. [d] In acetone-d_6 at room temperature.

methyl intermediates, the fragments $[(NP_3)Rh]^+$ and $[(PP_3)Rh]^+$.[1a,d] Finally, addition of KCN in MeOH to the latter 16-electron species yields 1 or 2 in excellent yields.

$$[(L)RhH] + MeOSO_2CF_3 \xrightarrow{-CH_4} [(L)Rh]^+ \xrightarrow{+KCN} [(L)Rh(CN)] \quad (2)$$

Compounds 1 and 2 are stable both in the solid state and in deoxygenated solutions in which they behave as nonelectrolytes. The IR spectra exhibit strong $\nu(C{\equiv}N)$ bands at 2070 (1) and 2100 cm^{-1} (2). The $^{31}P\{^1H\}$ NMR spectrum of 1 (Table I) in the temperature range 173–300 K consists of a sharp doublet at 28.36 ppm [$J(PRh)$ = 155.4 Hz], thus indicating equivalence of the three terminal phosphorus atoms of NP_3 and an overall C_{3v} symmetry of the complex. Likewise, the phosphorus NMR spectrum of 2 shows a first-order AM_3X splitting pattern that does not change with the temperature. The low-field signal, centered at 152.07 ppm, appears as a doublet of quartets and is assigned to the bridgehead phosphorus atom of PP_3 as indicated by the large coordination chemical shift ($\Delta(P)$ = 166.2).[5] The upfield resonance consists of a doublet of doublets and is due to the three equivalent equatorial phosphorus atoms that are coupled to rhodium and to the apical phosphorus. On the basis of all of these data, it is reasonable to assign to 1 and 2 a TBP structure in which the cyanide ligand and the bridgehead atom of the tripodal ligand lie trans to each other in axial positions.

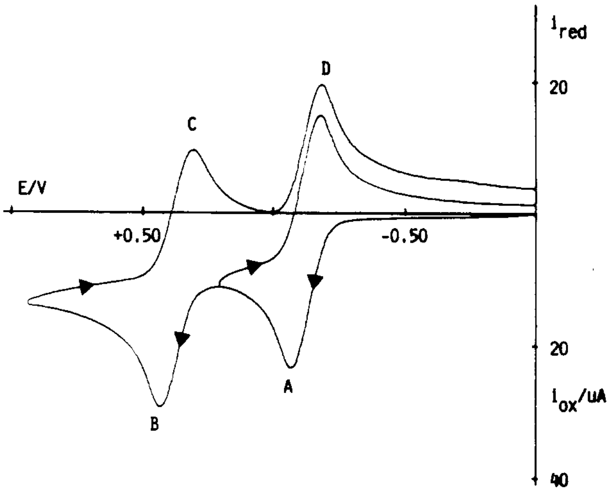

Figure 1. Cyclic voltammogram recorded at a platinum electrode on a CH_2Cl_2 solution containing 2 (1.5 × 10^{-3} mol dm^{-3}) and $[NBu_4]ClO_4$ (0.1 mol dm^{-3}). Scan rate = 0.2 V s^{-1}.

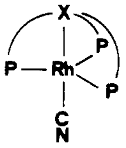

X = N, 1; P, 2

Electrochemistry. The cyclic voltammetric behavior exhibited by 2 in CH_2Cl_2 solution is shown in Figure 1. Two subsequent anodic processes (peaks A and B) are displayed, each of which showing a directly associated rereduction process in the reverse scan (peaks C and D, respectively). Controlled potential coulometric tests performed in correspondence of peak A (E_w = +0.1 V) and peak B (E_w = +0.7 V) show that each anodic step involves one electron per molecule of rhodium compound. Analysis[6] of the cyclic voltammetric responses relevant to the peak system A/D with scan rates varying from 0.02 to 10 V s^{-1} (at higher sweep rates, the response becomes ill-defined) provides evidence for an uncomplicated quasi-reversible one-electron oxidation ($i_{p(D)}/i_{p(A)}$ is constantly equal to unity; the difference $E_{p(A)} - E_{p(D)} = \Delta E_p$ increases from 80 to 300 mV; the current function $i_{p(A)}v^{-1/2}$ is substantially constant). We attribute this electron transfer to the Rh(I)/Rh(II) metal-centered redox change:

$$[(PP_3)Rh(CN)] \underset{+e}{\overset{-e}{\rightleftharpoons}} [(PP_3)Rh(CN)]^+$$

The stability of the monocationic species can be readily inferred from the cyclic voltammogram reported in Figure 2 which has been recorded on a CH_2Cl_2 solution of 2 after its exhaustive one-electron anodic macroelectrolysis at E_w = +0.1 V.

As far as the peak-system B/C is concerned, analysis of the relevant cyclic voltammograms with scan rates reveals that a relatively slow chemical reaction follows the quasi-irreversible Rh(II)/Rh(III) anodic step. In fact, the $i_{p(C)}/i_{p(B)}$ ratio increases from 0.85 at 0.02 V s^{-1} to 1.0 at 0.5 V s^{-1} (correspondingly, the ΔE_p term increases from 80 to 150 mV). As reported in Figure 3A, the cyclic voltammogram after the exhaustive two-electron oxidation

---

[5] Hohman, W. H.; Kountz, D. J.; Meek, D. W. *Inorg. Chem.* **1986**, *25*, 616. Grimley, E.; Meek, D. W. *Ibid.* **1986**, *25*, 2049. Meek, D. W.; Mazanec, T. J. *Acc. Chem. Res.* **1981**, *14*, 274.

[6] Brown, E. R.; Large, R. F. In *Physical Methods of Chemistry*; Weiss, A., Berger, A., Rossiter, B. W., Eds.; Wiley: New York, 1971; Part 11A.

Table II. Formal Electrode Potentials (in V vs SCE) for the Redox Changes Exhibited by Rh(I) Complexes of Formula $[(L)Rh(\sigma\text{-}R)]$ (L = NP_3, PP_3; R = CN, C≡CPh, $C≡CCO_2Et$)

	CH_2Cl_2		THF	
	$E^{\circ\prime}_{Rh(I)/Rh(II)}$	$E^{\circ\prime}_{Rh(II)/Rh(III)}$	$E^{\circ\prime}_{Rh(I)/Rh(II)}$	$E^{\circ\prime}_{Rh(II)/Rh(III)}$
$[(NP_3)Rh(CN)]$	−0.19	+0.23	−0.19[a]	+0.19[a]
$[(PP_3)Rh(CN)]$	−0.13	+0.38	−0.12	+0.34
$[(NP_3)Rh(C≡CPh)]$	−0.45	+0.02	−0.39	+0.02
$[[PP_3)Rh(C≡CPh)]$	−0.29	+0.38[b]	−0.27	+0.31
$[(NP_3)Rh(C≡CCO_2Et)]$	−0.21	+0.33	−0.18	+0.28

[a] Slightly double. [b] Peak potential value at 0.2 V s^{-1}.

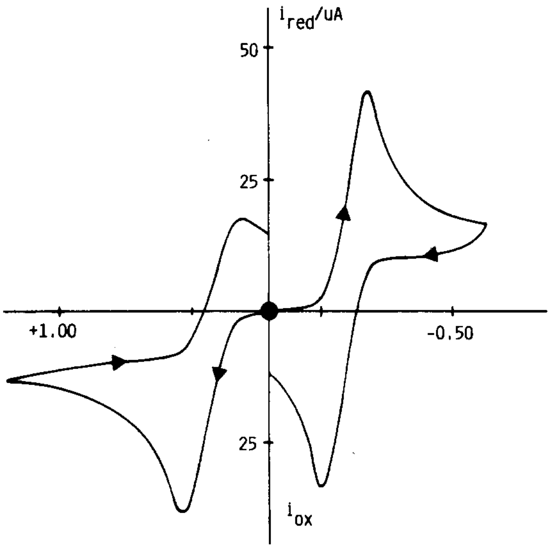

Figure 2. Cyclic voltammogram recorded at a platinum electrode on a CH_2Cl_2 solution containing **2** (4 × 10^{-3} mol dm^{-3}) after exhaustive one-electron oxidation at +0.1 V; supporting electrolyte $[NBu_4]ClO_4$ (0.1 mol dm^{-3}). Scan rate = 0.2 V s^{-1}. (●) Starting potential for cyclic scans.

of **2** (E_w = +0.8 V) shows the presence of ill-defined reduction processes apparently arising from products hardly correlable to the starting framework of **2**. Nevertheless, both the back-scan response in Figure 3A and the cyclic voltammogram recorded after the further exhaustive two-electron reduction (E_w = −1.2 V) of this solution (Figure 3B) indicate that the chemical complication which follows the second anodic step of **2** allows the compound to retain part of its complex framework (notice that the cyclic voltammogram shown in Figure 3B displays an oxidation pattern similar to the one reported in Figure 1 except for some additional minor peaks in the back-scan response due to unidentified species). Indeed, it is very likely that the short-lived species $[(PP_3)Rh(CN)]^{2+}$ degrades to the Rh(III) dicyano complex $[(PP_3)Rh(CN)_2]^+$ as shown in (3). In fact, the voltammogram of a pure

$$2[(PP_3)Rh(CN)]^{2+} \rightarrow [(PP_3)Rh(CN)_2]^+ + [(PP_3)Rh]^{3+} \qquad (3)$$

sample of $[(PP_3)Rh(CN)_2]BPh_4$[7] consists of an irreversible cathodic peak at E_p = −1.0 V.

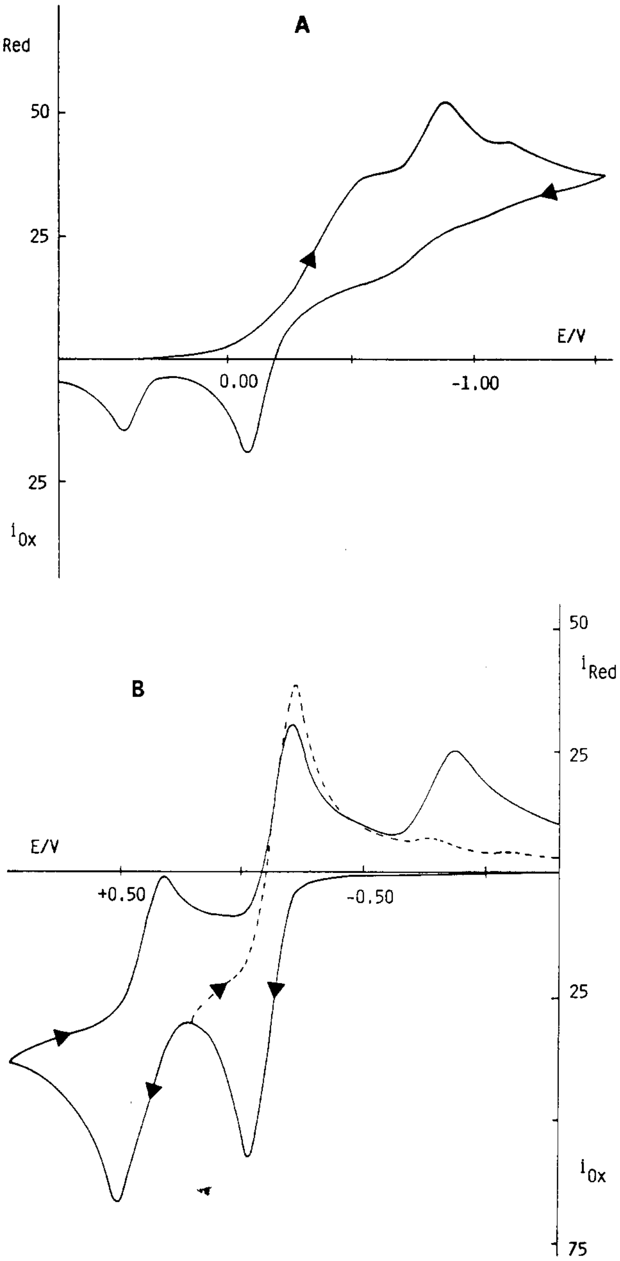

Figure 3. Cyclic voltammograms recorded at a platinum electrode on a CH_2Cl_2 solution containing **2** (5 × 10^{-3} mol dm^{-3}) and $[NBu_4]ClO_4$ (0.1 mol dm^{-3}) under the following experimental conditions: A, after exhaustive two-electron oxidation at +0.8 V; B, after the subsequent two-electron reduction at −1.2 V. Scan rate = 0.2 V s^{-1}.

The intermolecular reaction shown in (3) makes sense as one notes the strong electronic and coordinative unsaturation of the Rh(III) species $[(PP_3)Rh(CN)]^{2+}$. How the final dicyano complex may mechanistically form is hard to assess in the absence of intermediates; however, a dimerization pathway to give $[(PP_3)Rh(\mu\text{-}CN)_2Rh(PP_3)]^{4+}$ followed by decomposition to $[(PP_3)Rh(CN)_2]^+$ and $[(PP_3)Rh]^{3+}$ is a possible and palatable reaction.

---

(7) $[(PP_3)Rh(CN)_2]BPh_4$ was prepared as pale yellow crystals by stirring for 12 h an acetone solution of $[(PP_3)RhCl_2]Cl$[8] with a tenfold excess of methanolic KCN. Addition of *n*-hexane precipitated a clear yellow powder which was washed with methanol, water, ethanol, and light ether. The crude product was recrystallized by THF/ethanol mixture in the presence of $NaBPh_4$: yield 65%; IR ν(C≡N) 2140 cm^{-1} (m); $^{31}P\{^1H\}$ NMR (121.4 MHz, CD_2Cl_2, 298 K), AM_2QX pattern, $\delta(P_A)$ 143.94, $\delta(P_M)$ 52.30, $\delta(P_Q)$ 43.41 ppm, $J(P_AP_M) \simeq J(P_AP_Q)$ = 9.7 Hz, $J(P_MP_Q)$ = 18.1 Hz, $J(P_ARh)$ = 80.1 Hz, $J(P_MRh)$ = 93.6 Hz, $J(P_QRh)$ = 78.2 Hz.

(8) King, R. B.; Kapoor, R. N.; Saran, M. S.; Kapoor, P. N. *Inorg. Chem.* **1971**, *10*, 1851.

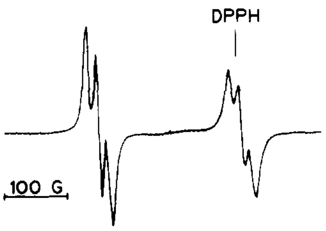

Figure 4. X-Band ESR spectrum of electrogenerated [(NP$_3$)-Rh(CN)]$^+$ in CH$_2$Cl$_2$ at 300 K.

The NP$_3$ derivative **1** displays an electrochemical behavior qualitatively similar to that of **2**, the only minor difference being an apparent higher rate of the chemical complication associated with the second step and leading to the dicyano complex [(NP$_3$)Rh(CN)$_2$]BPh$_4$.[9] Table II reports the formal electrode potentials of the redox changes for **1** and **2**. Change of solvent from CH$_2$Cl$_2$ to THF does not afford variations of the redox behavior. Also, Table II reports the redox parameters of the related σ-acetylide complexes [(NP$_3$)Rh(C≡CPh)] (**5**) and [(PP$_3$)Rh(C≡CR)] (R = Ph, **6**; R = CO$_2$Et, **7**).[1c,f] Interestingly, **5**, **6**, and **7** exhibit a cyclic voltammetric behavior essentially identical with that of **1** and **2** with the exception that the dicationic Rh(III) acetylides are now quite stable and isolable species. Given the close structural and chemical analogy between the five compounds, it is reasonable to conclude that the electronic properties of the cyanide and acetylide ligands make the difference. Actually, the two ligands are placed in the spectrochemical series near to each other and enter into π- and σ-bonding as well with transition metals.[11] However, in nice agreement with our findings, acetylide ligands, although slightly, are better donors, especially when high-valent metals are considered.[12] Certainly, much depends on the nature of the β-carbon substituent as shown by the almost concident values of $E^{\circ\prime}$ of **1** and **7** (the latter compound has a powerful electron-withdrawing substituent, namely, CO$_2$Et).

Precious information on the structure of the electrogenerated Rh(II) complex cations [(L)Rh(CN)]$^+$ is provided by ESR spectroscopy in solution. The spectrum on the NP$_3$ derivative in CH$_2$Cl$_2$ solution at 300 K (Figure 4) consists of a doublet of doublets of doublets centered at $\langle g\rangle$ = 2.066. The spectrum can be interpreted by using a $S = {}^1/_2$ spin Hamiltonian and has perfectly been simulated with three coupling constants to the phosphorus nuclei ($I = {}^1/_2$). The largest $\langle A_P\rangle$ value, 225.2 G, is typical of square-pyramidal (SQ) Rh(II) complexes in which the unpaired electron strongly interacts with the apical phosphorus atom as it looks at the d$_{z^2}$ SOMO.[1c,13]

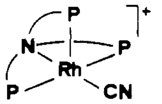

However, some distortion in the coordination polyhedron must be present since two different coupling constants, $\langle A_P\rangle$ = 19.0 and 13.2 G, have been used to simulate the interactions with the two basal phosphorus nuclei. The different line widths (2 G) of the two largely separated signals is due to the line-width dependence on the m_i value.[14] The line shape of the spectrum does not put in evidence any additional hyperfine structure most likely because of the coupling constants to rhodium are generally small (notice that the narrowest line width is 10.5 G).

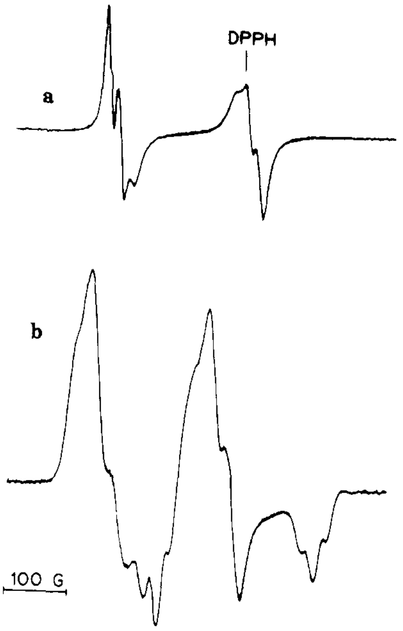

Figure 5. X-Band ESR spectra of electrogenerated [(PP$_3$)Rh-(CN)]$^+$ at 300 K (a) and 100 K (b).

The corresponding spectrum of the PP$_3$ derivative (Figure 5A) is much more complicated as it can be computed only considering the presence in the electrogenerated solution of [(PP$_3$)Rh(CN)]$^+$ of two isomeric Rh(II) species in ca. 1:0.7 ratio with $\langle g\rangle$ = 2.061 ($\langle A_P\rangle$ = 220.0, 18.5, and 7.5 G) and $\langle g\rangle$ = 2.066 ($\langle A_P\rangle$ = 205.0, 17.2, and 10.0 G), respectively. In contrast, the spectrum in CH$_2$Cl$_2$ glass at 100 K (Figure 5B) is consistent with the presence of a single species exhibiting SQ symmetry [$g_\perp$ (2.090) > $g_\parallel$ (2.004) $\simeq$ 2.000;[15] $A_\parallel$ = 242.0 G, $A_\perp$ = 188.2 G].[1c] A distorted three-line splitting in the parallel absorptions (21 G) is assigned to interaction with the two basal phosphorus nuclei (a similar but poorly resolved splitting can be envisaged also in the perpendicular absorptions). The frozen solution (CH$_2$Cl$_2$, 100 K) spectrum of [(NP$_3$)Rh(CN)]$^+$ is essentially identical with that of the PP$_3$ analogue, showing $g_\perp$ = 2.102, $g_\parallel$ = 2.002, $A_\perp$ = 203.0 G, and $A_\parallel$ = 280.5 G (see supplementary material).

Five-coordinate transition-metal complexes of PP$_3$ may adopt TBP or SQ geometries.[1d,16] Depending on the position of the fifth ligand, i.e. trans either to the bridgehead or to one terminal phosphorus atom, two different SQ structures are possible.

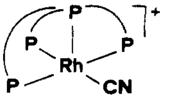

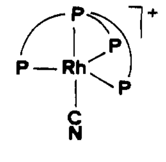

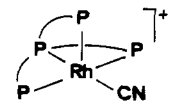

---

[9] [(NP$_3$)Rh(CN)$_2$]BPh$_4$ was synthesized analogously to the PP$_3$ derivative, using [(NP$_3$)RhCl$_2$]Cl[10] instead of [(PP$_3$)RhCl$_2$]Cl: yield 75%; IR ν(C≡N) 2120 cm^{-1} (w); ^{31}P{^{1}H} NMR (121.4 MHz, CD$_2$Cl$_2$, 298 K), AM$_2$X pattern, δ(P$_A$) 26.16, δ(P$_M$) 31.35 ppm, J(P$_A$P$_M$) = 24.7 Hz, J(P$_A$Rh) = 64.8 Hz, J(P$_M$Rh) = 82.8 Hz.

(10) Di Vaira, M.; Peruzzini, M.; Zanobini, F.; Stoppioni, P. *Inorg. Chim. Acta* **1983**, *69*, 37.

(11) (a) Nast, R. *Coord. Chem. Rev.* **1982**, *47*, 89. (b) Sharpe, G. A. In *Comprehensive Coordination Chemistry*; Wilkinson, G., Gillard, R. D., McCleverty, J. A., Eds.; Pergamon Press: Oxford, 1987; Vol. 2, Chapter 12.1.

(12) Gimarc, B. M. *Molecular Structure and Bonding*; Academic Press: New York, 1979.

(13) Bianchini, C.; Meli, A.; Laschi, F.; Vizza, F.; Zanello, P. *Inorg. Chem.*, in press.

(14) Wilson, R.; Kivelson, D. J. *J. Chem. Phys.* **1966**, *44*, 4445.

(15) Bencini, A.; Gatteschi, D. *Transition Met. Chem. (N.Y.)* **1982**, *8*, 1.

(16) Sacconi, L.; Mani, F. *Transition Met. Chem. (N.Y.)* **1982**, *8*, 179.

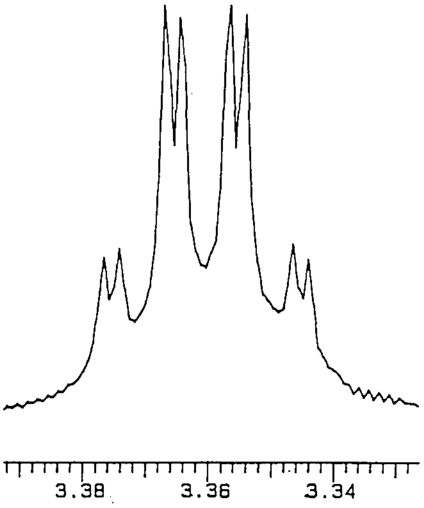

Figure 6. NMR signal for the methyl hydrogens of 8 (300 MHz, 298 K, CD_2Cl_2, TMS reference).

In the present Rh(II) case, the TBP structure is certainly to rule out because of Jahn–Teller distortion due to one electron in an *e* orbital of a threefold symmetry system.[17] Accordingly, it is reasonable to conclude that $[(PP_3)Rh(CN)]^+$ interconverts in ambient-temperature solutions between distorted SQ complexes with a rate which is slower than the ESR time scale. At this stage, however, it is not possible to draw any detailed conclusion about the type of the distortion in these species.

Nucleophilic Properties of 1 and 2. Reactions with $CH_3OSO_2CF_3$. The cyano complexes 1 and 2 react with a slight excess of $CH_3OSO_2CF_3$ to form a yellow solution from which air-stable crystals of $[(NP_3)Rh(CNMe)]BPh_4$ (**8**) and $[(PP_3)Rh(CNMe)]BPh_4$ (**9**), respectively, can be obtained upon addition of ethanol and $NaBPh_4$ (eq 4).

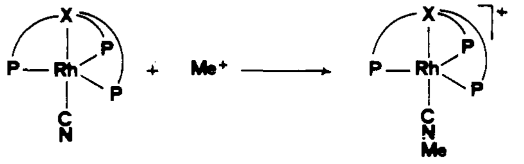

(4)

X = N, **8**; P, **9**

Compounds **8** and **9** are soluble in common organic solvents in which they behave as 1:1 electrolytes. The IR spectra still contain medium-intensity absorptions in the ν(C≡N) region at 2160 and 2150 cm^{-1}, respectively. The typical IR bands of the BPh_4^- counteranion are also present. The $^{31}P\{^1H\}$ NMR spectra (Table I), exhibiting splitting patterns of the A_3X and AM_3X types are diagnostic for TBP geometries. The ^1H NMR spectra of both compounds contain resonances at 3.36 (**8**) (Figure 6) and 3.33 ppm (**9**), each of which corresponding to 3 H. These resonances, which are not present in the spectra of 1 and 2, appear as quartets of doublets originated by long-range coupling to rhodium [^4J(HRh) = 0.8 Hz (**8**), 0.7 Hz (**9**)] and to the three basal phosphorus atoms [^5J(HP) = 3.0 Hz (**8**), 2.7 Hz (**9**)]. All of these data are consistent with electrophilic attack by the methyl cation at the nitrogen atom of the cyano groups to give TBP Rh(I) complexes with σ-bonded methyl isocyanide. Alkylation at nitrogen of σ-cyanide ligands has previously been reported only for a very few complexes of iron and ruthenium.[18]

Just to rule out any isomerization reaction leading to MeCN derivatives, we have synthesized and characterized the complexes $[(NP_3)Rh(NCMe)]BPh_4$ (**10**) and $[(PP_3)Rh(NCMe)]BPh_4$ (**11**) via addition of acetonitrile to THF solutions of the 16-electron fragments $[(NP_3)Rh]^+$ and $[(PP_3)Rh]^+$ (eq 5).[1a,d]

$$[(L)RhH] + Me^+ \rightarrow [(L)Rh]^+ \xrightarrow{MeCN} [(L)Rh(NCMe)]^+ \qquad (5)$$

As natural, **10** and **11** exhibit spectroscopic properties qualitatively similar to those of **8** and **9** (Table I). As an example, the ^1H NMR spectra contain resonances for the methyl protons of CH_3CN at 2.44 and 2.04 ppm which, in line with the results reported by DuBois and Miedaner,[19] appear as quartets [^5J(HP) = 2.6 Hz (**10**), 2.4 Hz (**11**)] because of coupling only to the cis phosphorus atoms of the tripodal ligands. In this respect, it is worth noticing that in **8** and **9**, the methyl protons are also coupled to rhodium. This may be taken as a diagnostic feature to discriminate between nitrile and isonitrile complexes of rhodium.

Reaction of 1 and 2 with $HOSO_2CF_3$. Compound **1** in CH_2Cl_2 reacts with a slight excess of triflic acid to give, after the addition of $NaBPh_4$ in ethanol, white crystals of $[(NP_3)Rh(H)(CN)]BPh_4$ (**12**) (eq 6). In contrast, protonation of **2** under the same conditions directly affords crystals of the cis hydrido cyanide complex $[(PP_3)Rh(H)(CN)](OSO_2CF_3)$ (**13**), following the addition of *n*-hexane. Compounds **12** and **13** are stable in the solid state and in deoxygenated solutions in which they behave as 1:1 electrolytes.

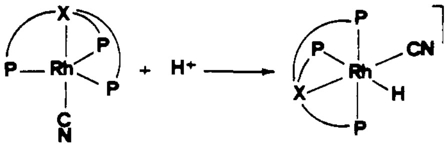

(6)

X = N, **12**; P, **13**

The presence of cis cyanide and hydride ligands in both compounds is clearly shown up by spectroscopic methods. The IR spectra exhibit broad absorbances at ca. 2000 cm^{-1} due to ν(Rh–H) and medium intensity bands at 2180 (**12**) and 2130 cm^{-1} (**13**) typical of σ-bonded cyanide groups. Well-resolved hydridic signals are observed in the high-field regions of the proton spectra. The experimental and computed spectra for the hydride resonances in **12** and **13** are reported in Figure 7. The multiplet in the spectrum of **12** appears as a doublet of doublets of triplets centered at −7.22 ppm (Figure 7A). This pattern stems from the strong coupling of the hydride to a phosphorus atom [$J(HP_{trans})$ = 166.9 Hz], to rhodium [J(HRh) = 13.7 Hz], and to the two basal phosphorus nuclei [$J(HP_{cis})$ = 6.9 Hz]. The hydride ligand can be readily located trans to phosphorus rather than to nitrogen on the basis of the large J(HP) value of 166.9 Hz.[1a,d] The analogous hydride resonance in the spectrum of **13** at −9.15 ppm consists of a doublet of doublets of quartets (Figure 7B). This multiplicity is originated by strong coupling to a trans phosphorus atom [$J(HP_{trans})$ = 152.5 Hz] and by additional coupling to rhodium [J(HRh) = 15.1 Hz] and to the three terminal phosphorus atoms of PP_3 which, although nonequivalent, exhibit fortuitous coincidence of the coupling constant to the hydride and, therefore, are responsible of the observed pseudoquartets [$J(HP_{cis})$ = 10.9 Hz]. The $^{31}P\{^1H\}$ NMR spectra showing canonical AM_2X (**12**) and AM_2QX (**13**) splitting patterns are consistent with OCT geometries.

---

[17] Jahn, H. A.; Teller, E. *Proc. R. Soc. London, Ser. A* **1937**, *161*, 220.
[18] Baird, G. J.; Davies, S. G. *J. Organomet. Chem.* **1984**, *262*, 215.
[19] DuBois, D. L.; Miedaner, A. *Inorg. Chem.* **1986**, *25*, 4642. DuBois, D. L.; Miedaner, A. *J. Am. Chem. Soc.* **1987**, *109*, 113.

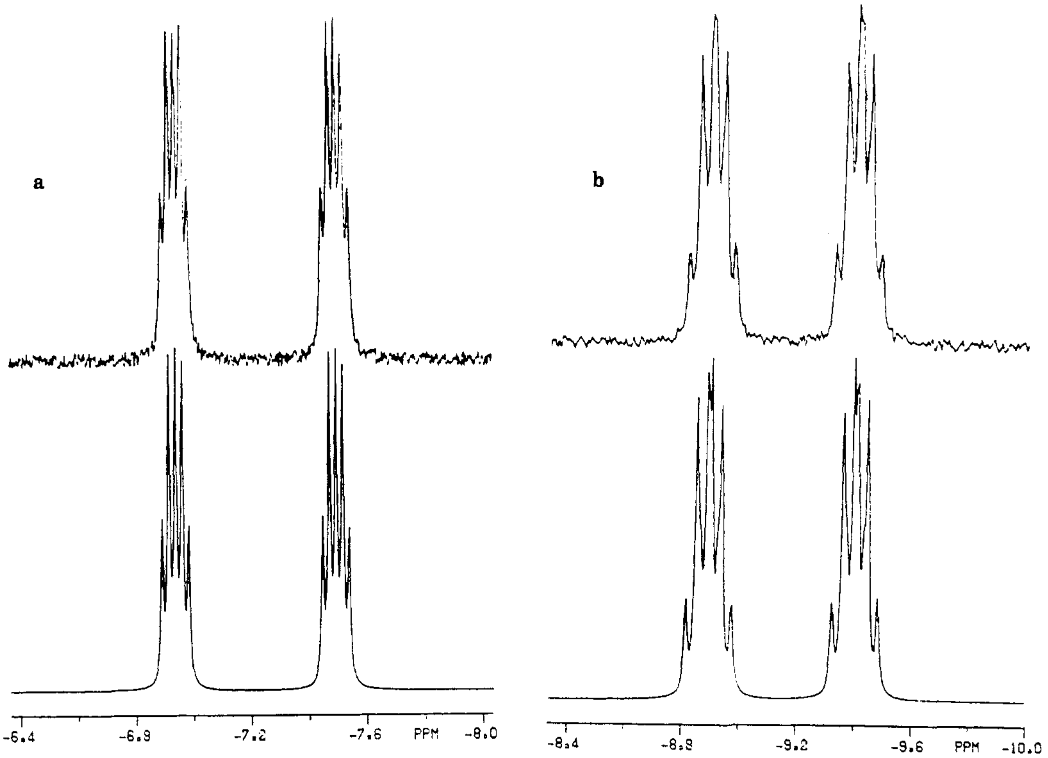

Figure 7. Experimental (top) and computed (bottom) ^1H NMR spectra (300 MHz, 298 K, CD_2Cl_2, TMS reference) in the hydride region of **12** (a) and **13** (b).

Despite the cyanide ligand is a strong-field ligand[11b] and, therefore, potentially able to stabilize metal to hydrogen bonds, cyanide hydride complexes of transition metals are still very rare compounds.[20] Actually, the only well-characterized compounds of this type, besides the homoleptic OCT $[MH(CN)_5]^{3-}$ (M = Co, Rh, Ir) trianions,[21] are the neutral complexes $[NiH(PR_3)_3(CN)]$ described by Tolman and co-workers.[22] On the basis of NMR spectroscopy, these compounds were assigned a TBP structure with the hydride and cyanide ligands located trans to each other in axial positions. Invariably, all the known examples of cyanide hydride complexes were obtained by oxidative addition of HCN to electron-rich Ni(0) or M(I) (M = Co, Rh, Ir) substrates. This route is an accessible one also for **12** and **13** by using the 16-electron fragments $[(NP_3)Rh]^+$ and $[(PP_3)Rh]^+$.

Conclusions

Two nucleophilic sites, namely, the rhodium center and the nitrogen atom of the cyano group, are present in the σ-cyanide complexes **1** and **2**; therefore, at least in principle, the reactions with electrophiles may take place either at the metal or at the ligand. In actuality, the reactions are controlled by the nature of the electrophilic reagent. In particular, since the formation of Rh–H and N–C bonds prevails over that of Rh–C and N–H bonds when **1** and **2** are reacted with H^+ or Me^+, the enthalpic contribution appears predominant in determining the course of the reactions.

The key step of homogeneous catalytic hydrocyanation of alkenes involves the oxidative addition of HCN to metal systems to give cis hydride cyanide intermediates.[23] These undergo insertion of alkene into M–H bonds to form alkyl cyano complexes which reductively eliminate the nitrile, thus restoring the metal catalyst. Within this context, the cis hydride cyanide complexes **12** and **13** deserve a particular attention. Their stability together with the propensity of the $[(NP_3)Rh]^+$ and $[(PP_3)Rh]^+$ fragments to undergo reversible oxidative addition/reductive elimination pathways under very mild conditions[1] makes **12** and **13** potentially amenable compounds for detailed studies on catalytic hydrocyanation of alkenes.

Experimental Section

All the reactions and manipulations were routinely performed under a nitrogen atmosphere using standard Schlenk techniques. Tetrahydrofuran was purified by distillation over $LiAlH_4$ under nitrogen just prior to use. *n*-Hexane was dried over sodium and distilled immediately before using. All other solvents and reagents were reagent grade and were used as received from commercial suppliers. Ethyl cyanoformate was obtained from Aldrich. Infrared spectra were recorded on a Perkin-Elmer 283 spectrophotometer using samples mulled in nujol between CsJ plates. Proton NMR spectra were recorded at 300 MHz on a Varian VXR 300 spectrometer. Peak positions are relative to tetramethylsilane as an internal reference. $^{31}P\{^1H\}$ NMR spectra were recorded on Varian CFT20 and Varian VXR 300 instruments operating at 32.19 and 121.42 MHz, respectively. Chemical shifts are relative to 85% H_3PO_4 as an external reference with downfield values assumed as positive. Conductivities were measured with a WTW Model LBR/B conductivity bridge. The conductivity data were obtained at a sample concentrations of ca. 1×10^{-3} M in nitroethane solutions. The proton NMR spectra in the high-field region of the cis hydrido cyanide complexes **12** and **13** were simulated by use of an updated version of LAOCN3 program.[24] The materials

---

(20) Moore, D. S.; Robinson, S. D. *Chem. Soc. Rev.* **1983**, *12*, 415.

(21) Griffith, W. P.; Pratt, L.; Wilkinson, G. *Nature (London)* **1958**, *182*, 466. Baranowskii, I. B. *Zh. Neorg. Khim.* **1978**, *23*, 2579; *Russ. J. Inorg. Chem. (Engl. Transl.)* **1978**, *23*, 1429. Jewsbury, R. A.; Maher, J. P. *J. Chem. Soc., Dalton Trans.* **1972**, 2089.

(22) Druliner, J. D.; English, A. D.; Jesson, J. P.; Meakin, P.; Tolman, C. A. *J. Am. Chem. Soc.* **1976**, *98*, 2156.

(23) Brown, E. S. In *Organic Synthesis via Metal Carbonyls*; Wender, I., Pino, P., Eds.; Wiley: New York, 1977; Vol. 2, p 655. James, B. R. In *Comprehensive Organometallic Chemistry*; Wilkinson, G., Stone, F. G. A., Abel, E. W., Eds.; Pergamon Press: Oxford, 1982; Vol. 8, Chapter 51.2.

(24) Castellano, C.; Bothner-By, A. A. *J. Chem. Phys.* **1964**, *41*, 3863.

and the apparatus used for the electrochemical experiments have been described elsewhere.[25] The potential values are relative to an aqueous calomel electrode (SCE). The temperature was controlled at 20 ± 0.1 °C. Under the present experimental conditions the ferrocenium/ferrocene couple was located at +0.49 V in CH_2Cl_2 solution and at +0.56 in THF solution. X-band EPR spectra were recorded with an ER 200-SRCB Bruker spectrometer operating at w_0 = 9.78 GHz. The control of the external magnetic field was obtained with a microwave bridge ER 041 MR Bruker wavemeter. The temperature was varied and controlled with an ER 4111 VT Bruker device with an accuracy of ±1 °C. In order to estimate accurate g_{iso} and g_{aniso} values over the temperature range of interest, the diphenylpicrylhydrazyl (DPPH) free radical was used as field marker (g_{iso}(DPPH) = 2.0036). In order to assure quantitative reproducibility, the samples were placed into calibrated quartz capillary tubes permanently positioned in the resonance cavity. GC analyses were performed on a Shimadzu GC-8A gas chromatograph fitted with a thermal conductivity detector and a 6-ft 0.1% SP-1000 on Carbopack C $^1/_8$ in. stainless-steel column (Supelco Inc.). Quantification was achieved with a Shimadzu C-R6A Chromatopac coupled to the chromatograph, operating with an automatic correct area normalization method.

All the solid compounds were usually collected on sintered glass frits and washed, unless otherwise stated, with ethanol and *n*-pentane before being dried in a stream of nitrogen. *Caution. KCN and HCN are extremely toxic and should be used only in a well-ventilated hood. Heavy rubber gloves should be worn and any contact with skin or clothing carefully avoided.*

Preparation of [(NP$_3$)Rh(CN)] (1). Method A. To a stirred suspension of 3 (600 mg, 0.8 mmol) in THF (40 ml) were added 0.5 mL of neat ethyl cyanoformate (6.92 mmol). The resulting slurry was heated gently to ca. 40 °C or 1 h. During this time the starting yellow microcrystals dissolved to produce a light yellow solution, which was cooled to room temperature. Addition of an ethanol/*n*-hexane mixture (1:1 v/v, 30 mL) and concentration under a brisk current of nitrogen allowed 1 to separate as light yellow crystals. Yield: 450 mg (71%). The formation of ethyl formate in 85% yield was determined by GC.

Method B. A suspension of 3 (600 mg, 0.8 mmol) in THF (40 mL) was treated with a slight excess of $MeOSO_2CF_3$ (114 μL, 1.00 mmol) at 0 °C under magnetic stirring. In a few minutes the starting yellow compound dissolved to give a colorless solution. Addition of KCN (80 mg, 1.23 mmol) in CH_3OH (15 ml) caused the solution to become light yellow. Yellow crystals of 1 separated upon addition of ethanol (30 mL). Yield: 570 mg (90%). IR: ν(C$\equiv$N) 2070 cm^{-1} (s). Anal. Calcd for $C_{43}H_{42}N_2P_3Rh$: C, 65.99; H, 5.41; N, 3.58; Rh, 13.15. Found: C, 65.46; H, 5.57; N, 3.49; Rh, 13.01.

Preparation of [(PP$_3$)Rh(CN)] (2). Method A. Neat $NCCO_2Et$ (0.35 mL, 4.84 mmol) was pipetted into a THF (20 mL) solution of 4 (400 mg, 0.52 mmol). The resulting solution was heated at ca. 40 °C for 20–30 min and then cooled to room temperature. Addition of ethanol/*n*-hexane (1:1 v/v, 30 mL) and concentration under a stream of nitrogen yielded light yellow microcrystals of 2. Yield: 295 mg (70%). The formation of ethyl formate in 80% yield was determined by GC.

Method B. A CH_3OH solution (10 mL) of KCN (40 mg, 0.61 mmol) was added to a THF solution (20 mL) of 4 (400 mg, 0.52 mmol) which has been treated with a slight excess of $MeOSO_2CF_3$ (70 μL, 0.61 mmol). Addition of ethanol (25 mL) and concentration of the resulting solution gave 2. Yield: 360 mg (84%). IR: ν(C$\equiv$N) 2100 cm^{-1} (s). Anal. Calcd for $C_{43}H_{42}NP_4Rh$: C, 64.59; H, 5.28; N, 1.75; Rh, 12.87. Found: C, 64.12; H, 5.30; N, 1.66; Rh, 12.46.

Preparation of [(NP$_3$)Rh(CNMe)]BPh$_4$ (8). A suspension of 1 (200 mg, 0.26 mmol) in 15 mL of THF was treated at 0 °C under vigorous stirring with 35 μL (30 μmol) of neat $MeOSO_2CF_3$. In few minutes the starting yellow cyanide dissolved yielding a yellow solution. On addition of solid $NaBPh_4$ (200 mg, 0.60 mmol) and ethanol (20 mL) canary yellow crystals separated. Yield: 230 mg (79%). Λ_M = 55 Ω^{-1} cm^2 mol^{-1}. IR: ν(C$\equiv$N) 2150 cm^{-1} (m). Anal. Calcd for $C_{68}H_{65}BN_2P_3Rh$: C, 73.13; H, 5.87; N, 2.51; Rh, 9.21. Found: C, 72.87; H, 5.93; N, 2.44; Rh, 9.09.

Preparation of [(PP$_3$)Rh(CNMe)]BPh$_4$ (9). The methyl isocyanide derivative of the PP$_3$ ligand, 9, was prepared by the same procedure used for 8, using 2 instead of 1. Yield: 190 mg (67%). Λ_M = 53 Ω^{-1} cm^2 mol^{-1}. IR: ν(C$\equiv$N) 2150 cm^{-1} (br). Anal. Calcd for $C_{68}H_{65}BNP_4Rh$: C, 72.03; H, 5.78; N, 1.23; Rh, 9.08. Found: C, 71.77; H, 5.89; N, 1.19; Rh, 9.00.

Preparation of [(NP$_3$)Rh(NCMe)]BPh$_4$ (10). To a suspension of 1 (200 mg, 0.27 mmol) in 20 mL of THF was added via syringe $MeOSO_2CF_3$ (33 μL, 0.30 mmol). In a few minutes the starting yellow compound dissolved to give a colorless solution. Addition of neat acetonitrile (1.00 mL, 19.10 mmol) caused the colorless solution to become red. Red crystals were obtained after addition of solid $NaBPh_4$ (300 mg, 0.88 mmol) and ethanol (20 ml). Yield: 290 mg (96%). Λ_M = 57 Ω^{-1} cm^2 mol^{-1}. IR: ν(C$\equiv$N) 2275 cm^{-1} (vw). Anal. Calcd for $C_{68}H_{65}BN_2P_3Rh$: C, 73.13; H, 5.87; N, 2.51; Rh, 9.21. Found: C, 73.06; H, 6.01; N, 2.39; Rh, 9.17.

Preparation of [(PP$_3$)Rh(NCMe)]BPh$_4$ (11). The acetonitrile derivative 11 was obtained as yellow microcrystals following the above procedure, using 4 instead of 3. Yield: 275 mg (93%). Λ_M = 52 Ω^{-1} cm^2 mol^{-1}. IR: ν(C$\equiv$N) 2150 cm^{-1} (br, s). Anal. Calcd for $C_{68}H_{65}BNP_4Rh$: C, 72.03; H, 5.78; N, 1.23; Rh, 9.08. Found: C, 71.76; H, 5.69; N, 1.09; Rh, 8.79.

Preparation of [(NP$_3$)Rh(H)(CN)]BPh$_4$ (12). Method A. Neat $HOSO_2CF_3$ (30 μL, 0.34 mmol) was syringed into a solution of 1 (240 mg, 0.31 mmol) in CH_2Cl_2 (25 mL) at 0 °C. The originally light yellow color immediately faded. On addition of ethanolic (20 mL) $NaBPh_4$ (300 mg, 0.88 mmol) white crystals of 12 separated. Yield: 200 mg (58%).

Method B. Gaseous hydrogen cyanide was bubbled into a THF solution (30 mL) of [(NP$_3$)Rh]$^+$ prepared in situ as previously described [3, 460 mg (0.62 mmol); $MeOSO_2CF_3$, 82 μL (0.70 mmol)]. On addition of ethanol (30 mL) and solid $NaBPh_4$ (300 mg, 0.88 mmol) white crystals of 12 separated. Yield: 320 mg (93%). Λ_M = 59 Ω^{-1} cm^2 mol^{-1}. IR: ν(C$\equiv$N) 2180 cm^{-1} (m); ν(Rh—H) 1990 cm^{-1} (br). Anal. Calcd for $C_{67}H_{63}BN_2P_3Rh$: C, 72.97; H, 5.76; N, 2.54; Rh, 9.33. Found: C, 72.40; H, 5.91; N, 2.36; Rh, 9.27.

Preparation of [(PP$_3$)Rh(H)(CN)](OSO$_2$CF$_3$) (13). Method A. A solution of 2 (200 mg, 0.25 mmol) in CH_2Cl_2 (25 mL) was treated with a slight excess of $HOSO_2CF_3$ (22 μL, 0.30 mmol) at 0 °C. The originally yellow solution turned immediately colorless. Additon of two volumes (50 mL) of cold *n*-hexane precipitated white microcrystalline crystals of 13. The product was collected by filtration and washed twice with *n*-pentane (2 × 20 mL) before being dried in a nitrogen stream. Yield: 200 mg (84%).

Method B. 13 was prepared in ca. 70% yield by reacting gaseous HCN with a THF solution of [(PP$_3$)Rh]$^+$ as described above for 12. IR: ν(C$\equiv$N) 2130 cm^{-1} (m); ν(Rh—H) 1980 cm^{-1} (br). Anal. Calcd for $C_{44}H_{43}F_3NO_3P_4RhS$: C, 55.65; H, 4.56; N, 1.47; Rh, 10.84. Found: C, 57.06; H, 4.69; N, 1.11; Rh, 10.37.

Registry No. 1, 118681-53-1; 2, 118681-54-2; 3, 85233-91-6; 4, 109786-30-3; 8, 118713-48-7; 9, 118681-56-4; 10, 118713-50-1; 11, 118681-58-6; 12, 118681-60-0; 13, 118681-62-2; $MeOSO_2CF_3$, 333-27-7; $NCCOOCH_2CH_3$, 623-49-4; [(NP$_3$)Rh(CN)]$^+$, 118681-63-3; [(PP$_3$)Rh(CN)]$^+$, 118681-64-4; [(NP$_3$)Rh(CN)]$^{2+}$, 118681-65-5; [(PP$_3$)Rh(CN)]$^{2+}$, 118681-66-6; [(PP$_3$)Rh(CN)$_2$]BPh$_4$, 118681-68-8; [(NP$_3$)Rh(CN)$_2$]BPh$_4$, 118681-70-2; [(PP$_3$)RhCl$_2$]Cl, 118681-71-3; [(NP$_3$)RhCl$_2$]Cl, 85233-84-7; CN$^-$, 57-12-5.

Supplementary Material Available: X-Band ESR spectra of electrogenerated [(NP$_3$)Rh(CN)]$^+$ in CH_2Cl_2 at 300 and 100 K (1 page). Ordering information is given on any current masthead page.

---

[25] Bianchini, C.; Mealli, C.; Meli, A.; Sabat, M.; Zanello, P. *J. Am. Chem. Soc.* 1987, *109*, 185.